arXiv:astro-ph/0702274v1 9 Feb 2007

Constraints on accretion in Ultraluminous X-ray Sources from *Spitzer* IRS observations of NGC 4485/90: Infrared diagnostic diagrams

Gerardo A. Vázquez
Physics & Astronomy Department, Johns Hopkins University, Baltimore, MD 21218
vazquez@pha.jhu.edu

Ann E. Hornschemeier
NASA/GSFC, Code 662, Laboratory for X-ray Astrophysics Greenbelt, MD 20771
annh@milkyway.gsfc.nasa.gov

Edward Colbert
Physics & Astronomy Department, Johns Hopkins University, Baltimore, MD 21218
colbert@jhu.edu

Timothy P. Roberts and Martin J. Ward
Dept. of Physics, Durham University, South Road, Durham DH1, 3LE, UK
t.p.roberts@durham.ac.uk, m.ward@durham.ac.uk

Sangeeta Malhotra
Arizona State University, Department of Physics & Astronomy, P.O. Box 871504 Tempe, AZ 85287-1504
sangeeta.malhotra@asu.edu

ABSTRACT

Constraining the astrophysical nature of Ultra-Luminous X-ray (ULX) sources, which have X-ray luminosities exceeding 10^{39} erg s^{-1}, has been elusive due to the optical faintness of any counterparts. With high spectral resolution observations in the $\sim$ 10–30μm wavelength range we have conducted an experiment to study six ULX sources in the NGC 4485/90 galaxy pair. We have found that five of the six ULXs, based on mid-infrared spectral diagnostics, show the characteristic higher ionization features that are found in AGN. The sixth source, ULX-1, is consistent with being a supernova remnant. The chief infrared spectral diagnostics used are the ratios of [S III]/[Si II] *vs* [Ne III]/[Ne II]. In two instances fits to the continuum and *poly aromatic hydrocarbons* (PAH) features also indicate higher dust temperatures that are characteristic of accreting sources. Overall, however, we find the continuum is dominated by stellar processes, and the best diagnostic features are the emission lines. High spectral resolution studies in the mid-infrared thus appear to show great promise for determining the astrophysical nature of ULXs.

Subject headings: galaxies: general — ULRGS: individual(NGC 4485, NGC 4490)

1. Introduction

Ultra-Luminous X-ray sources (ULXs) are generally defined as extra-nuclear galactic X-ray sources with X-ray luminosities $L_{\rm X} \geq 10^{39}$ erg s^{-1}, a luminosity that is seldom reached by any Galactic (Milky Way) X-ray binary (XRB). If ULXs emit their X-rays isotropically, by Eddington arguments, the central object could be a black hole (BH) with mass M $\geq$ 5 M$_{\odot}$, and for Eddington ratios of $\sim 10^{-2}$–10^{-1}, the implied mass of the central object is $\sim$50–500 M$_{\odot}$. Therefore, some ULXs could be accreting intermediate-mass black holes (IMBHs, Colbert & Mushotzky 1999; Ptak & Griffiths 1999; Miller & Colbert 2004). The majority of ULXs, however, are likely accreting *stellar* mass black holes (e.g., $\sim$ 1–10 M$_{\odot}$) as there appears to be a strong association between ULX sources and star formation in galaxies (Zezas & Fabbiano 2002). One popular model claims that ULXs are merely stellar-mass BHs in high-mass XRBs, and mild beaming of their X-ray luminosities produces the observational illusion of extremely high X-ray luminosities (e.g., King et al. 2001; King 2006). Hundreds of ULXs are known at the present time (e.g., Roberts & Warwick 2000, Colbert & Ptak 2002, and Chandra ULX catalogs by Ptak et al.[1], Swartz et al. 2004, and Liu & Bregman 2005).

Accreting binaries such as these could be precursors to eventual gravitational radiation events. Further, ULXs are important as they often dominate the total observed X-ray flux in starburst galaxies (see Colbert et al. 2004). Their relationship with star formation also appears to extend to cosmologically interesting ($z \gtrsim 0.1$) look-back times (Hornschemeier et al. 2004; Lehmer et al. 2006) and may provide a cosmological tool.

Unfortunately, all but the very brightest ULX sources are too faint for detailed X-ray spectroscopy studies (the best cases must rely upon resolving power of R= 60 at 6.4 kev, available with X-ray CCDs; Miller et al. 2004).

There is perhaps hope for ascertaining the nature of ULX sources by studying their interactions with their surroundings, such as gas, dust and stars; such information may be captured using infrared spectral diagnostics. Genzel et al. (1998) were the first to show that ionization-sensitive indices based on mid-infrared ratios were helpful for identifying the nature of heavily obscured nuclear sources (Genzel et al. 1998; Laurent et al. 2000; Sturm et al. 2002; Peeters, Spoon, & Tielens 2004b). We have thus taken advantage of the resolving power (R $\sim$ 600) of the *Infrared Spectrograph* (IRS) on board the *Spitzer Space Telescope* (SST) to calculate highly accurate ionization diagnostic ratios.

The nearby galaxy pair NGC 4485/90 provides an excellent opportunity for studying ULX sources (see Roberts et al. 2002). There are six ULXs in NGC 4485/90 (D = 7.8 Mpc, Tully 1998), far more than is typical ($\leq$ 2 in most cases, and 0.2, on average; Colbert & Ptak 2002; Ptak & Colbert 2004). The unprecedented sensitivity and angular resolution afforded by the *Spitzer* Space Telescope's Infrared Spectrograph (IRS) coupled with the proximity of NGC 4485/90 allow us to carry out this important experiment.

2. IRS spectroscopy: Observing strategy and Reduction

We have performed spectral mapping of the system NGC 4485/90 by using the mapping mode of the IRS (Houck et al. 2004) on board the SST. Rectangular regions of $11\farcs1\times22\farcs3$ and $4\farcs7\times11\farcs3$ (i.e. zones of $\sim$ 0.42 $\times$ 0.84 kpc and $\sim$ 0.18 $\times$ 0.42 kpc at the system) were mapped using both the short-high (SH, $\sim 9.9 - 19.7$ μm) and long-high (LH, $\sim 19.5 - 38$ μm) slits, respectively. Six rectangular regions centered at the positions of the ULXs (Table 1) were covered using a 1×4 and 1×7 grid array for the long and and short slits of the IRS. In addition two positions in NGC 4490 that are *not* near ULXs were observed with the same configuration as the one used for the ULXs. The integration time was 240 s at each position, and the step size is half the slit width perpendicular to the slit. This configuration allows net exposures of $\geq$ 480 s for rectangular sizes 16.7×22.3" and 14.1×11.3" for long and short high slits, respectively.

Sets of 8 exposures were taken for each position with the IRS. The pre-reduced basic calibrated data (*bcd*) files were obtained from the *Spitzer Science Center* (SSC) data base. In order to extract the spectra for the SH and LH modes,

[1]URL: http://www.xassist.org

we used SMART (Spectroscopy Modeling Analysis and Reduction, Higdon et al. 2004) which is publicly available software provided by the SSC[2].

3. Infrared Spectral Diagnostics

We have used line identifications from Smith et al. (2004), Armus et al. (2006) and NIST[3] (Martin et al. 1995). We have combined both modes by re-scaling the LH mode spectra to the SH mode spectra by adding or subtracting a constant and then re-binning to a resolution of 0.0287 μm/pixel. In Fig. 1 we show the combined spectra from all the positions.

As we can see from Fig. 1, some of the line features are present or stronger in the ULX region than in the comparison region spectra. The most striking examples are features such as [S IV]10.51, [Ne II]12.81, [Na I]14.6, [Ne III]15.55, [S III]18.71, and [S III]33.48 μm that seem to be significantly stronger in the comparison regions and ULX-1(which is thought to be a SNR rather than an accreting binary), than in the rest of the sources. In the opposite way, the [Si II]34.82 μm line is stronger in ULX-2 to ULX-6.

The purpose of this work is to generate some emission line diagnostic diagrams similar to commonly used optical emission line diagrams, which have proven useful in separating accretion-dominated sources from those dominated by stellar sources (e.g., Baldwin, Phillips & Terlevich 1981; Kauffmann et al. 2006, and references therein). A popular mid-infrared diagnostic first put forth in an ISO spectroscopic survey of ultra-luminous infrared galaxies (ULIRGs) by Genzel et al. (1998), and later explored by Peeters, Spoon, & Tielens (2004b), plots the emission line ratio [O IV]25.91 μm / [Ne II]12.81 μm versus the strength of a mid-infrared *poly aromatic hydrocarbons* (PAH) features. These two lines however, are relatively weak and difficult to detect in lower luminosity systems. Taking advantage of the strong low ionization line emission of [Si II]34.82 μm, Dale et al. (2006) suggested alternative diagrams to distinguish AGNs from SF regions such as [Ne III]15.55μm/[Ne II]12.81μm and [S III]33.48μm/[Si II]34.82μm. These ratios proved to be successful in separating accretion-powered vs. SF powered regions in the SINGS galaxy sample.

We have calculated these ratios for our eight spectra, shown in Fig. 2. We have also plotted the data from Dale et al. (2006) that include nuclear and extra-nuclear regions from SINGS, the SMC/LMC and galactic H II regions. Errors in the emission line fluxes calculation are around 10%. The boundaries in Fig. 2 are defined with the same curves as in Dale et al. (2006). As we can see from Fig. 2, ULX-2, ULX-3, ULX-4, ULX-5, and ULX-6 are in zone I where Seyfert and Liners are observed, while ULX-1, comp-NW, and comp-CENT are located in zone III as star forming systems. For ULX-2 and ULX-6 the line ratio [S III]33.48 μm/[Si II]34.82 μm is < 0.01, which is extremely low compared with extragalactic objects in Fig. 2.

The SINGS group has recently developed models (*pahfit*, Smith et al. 2007) to characterize PAH features. The models include starlight continuum, featureless thermal dust continuum, pure rotational lines of H_2, fine-structure lines, dust emission features, and dust extinction. The starlight continuum is represented by a blackbody emission was fixed at $T_\star = 5000$ K. Nine thermal dust continuum components are represented by blackbodies at fixed temperatures $T_{\rm m} = 35, 50, 75, 90, 110, 135, 200, 300, 500$ K. The program *pahfit* performs a fit through two hundred iterations, each iteration determines a χ^2 value for all nine temperatures, until a minimum value for χ^2 is found. Dust temperatures are based on the shape of the continuum spectrum. We show the corresponding fits in Table 1, where we show ULX-2 and ULX-6 have hotter components, but the relative intensity of those components is low for ULX-1.

The presence of a hotter dust component will flatten the spectra for our range of wavelengths. This effect is seen in Fig 1 for ULX-2 and ULX-6.The rest of the parameters modeled will be subject of a forthcoming paper (Vázquez, et al. 2007b, *in preparation*).

Finally, we have found a strong linear anti-correlation between the observed $\log(L_{\rm X})$ and $\log$([S III]33.48 μm/[Si II]34.82 μm). The regression and intercept coefficients are -0.21 ± 0.05 and 39.09 ± 0.6, respectively with a RMS = 0.08.

[2]http://ssc.spitzer.caltech.edu/archanaly/contributed/smart/

[3]Available at http://physics.nist.gov/cgi-bin/AtData/main_asd/

4. Discussion

For the first time the IR continuum and lines ($\sim 9.9 - 38$ μm) have been observed in ULXs by using the power of the *Spitzer* IRS. It is likely that this ULXs are irradiating nearby star-forming clouds. Although the geometry is probably thus quite complex, we do find some hints of information on the underlaying X-ray radiation. The most striking result from the data analyzed in this work is the one in Fig. 2, which shows that five of the six ULXs reported by Roberts et al. (2002) fall in the "AGN zone" determined by the infrared diagnostic emission line ratios defined by the emission lines of Ne, S, and Si (Dale et al. 2006). Both of the comparison regions used here, which do not harbor ULX sources, fall in the zone of SF. The SF zone is also occupied by extra-nuclear star-forming regions in the SINGS galaxy sample and SMC/LMC and galactic H II regions. The emission line at [N I]10.33 and other unidentified features also behave like [Si II]34.82 μm, showing a stronger contribution in ULX-2 to 6 than in ULX-1 and both of the comparison regions.

The presence of a hotter dust component in our PAH/continuum modeling (see Table 1), suggests that at least for ULX-2 and ULX-6 the [Si II] lines could be originating from an accreting source. A dilution factor could be affecting the rest of the ULXs possibly due to their location within their host galaxy. All of this is consistent with the anti-correlation we have found between the line emission ratio of [S III]33.48μm/[Si II]34.82μm and the observed X-ray luminosity of the six ULXs, the more luminous the sources the lower the ratio of these emission lines.

Different scenarios for the strong [Si II] line have been suggested in the literature. In these scenarios the increasing density in H II, photo-dissociation (PDR), and X-ray dissociation regions (XDR), respectively, increases the intensity of the [Si II]34.82 μm line (see Maloney, Hollenbach, & Tielens 1996; Kaufman et al. 2006; Meijerink & Spaans 2005). A third scenario suggests that heavy elements such as Si, Mg, and Fe may be returned to the gas phase by dust destruction (e.g., sputtering) in regions subject to strong shocks caused by stellar winds, starbursts, and AGN activity (Dale et al. 2006). Details of the geometry and ionization balance in the region require more detailed fitting, and also spatial mapping of spectral parameters as ULXs are thought to have drifted from their birthplaces. The origin of these lines could thus be disentangled with detailed IRS mapping observations and IRAC imaging, which are the subject of a forthcoming paper (Vázquez et al. 2007b).

With the exception of a weak detection in ULX-1, we have not detected the emission line [O IV]25.91 μm, this line is a strong feature in SNR (e.g., Morris et al. 2006; Williams, Chu, & Gruendl 2006), supporting previous suggestions that ULX-1 is a SNR (e.g., based on radio and X-ray constraints; Roberts et al. 2002).

The mid-infrared emission line diagnostics used to uncover the nature of AGNs and SF galaxies has been shown here to work well separating SFRs and young SN from probably true accreting ULXs (according to X-ray observations; Roberts et al. 2002). But this is a small sample of ULXs to claim a general rule that could be improved observing a higher number of ULXs. The present work shows that a new diagnostic window has been opened on ULXs and their immediate environment via important mid-infrared features like [Si II]34.82 μm, made observationally available by the extraordinary performance of the IRS on board the *Spitzer* Space Telescope.

Many thanks to Danny A. Dale who provided us his data for our figures. This work has been supported by the *Spitzer* grant 3360 (P.I. Colbert).

REFERENCES

Armus, L., et al. 2006, ApJ, 640, 204

Baldwin, J. A., Phillips, M. M., & Terlevich, R. 1981, PASP, 93, 5

Colbert, E., et al. 2004, ApJ, 602, 231

Colbert, E., & Mushotzky, R. 1999, ApJ, 519, 89

Colbert, E., & Ptak, A. 2002, ApJS, 143, 25

Dale, D. A. et al. 2006, ApJ, 646, 161

Genzel, R. et al. 1998, ApJ, 498, 579

Higdon, S. J. U., et al. 2004, PASP, 116, 975

Hornschemeier, A. E., et al. 2004, ApJ, 600, 147

Houck, J. R., et al. 2004, ApJS, 154, 18

Kaufman, M. J., Wolfire, M. G., & Hollenbach, D. J. 2006, ApJ, 644, 283

Kauffmann, G., Heckman, T. M., De Lucia, G., Brinchmann, J., Charlot, S., Tremonti, C., White, S. D. M., & Brinkmann, J. 2006, MNRAS, 367, 1394

King, A. R., et al. 2001, ApJ, 552, 109

King, A. R. 2006, in Compact stellar X-ray sources. Edited by Walter Lewin & Michiel van der Klis. Cambridge Astrophysics Series, No. 39. Cambridge, UK: Cambridge University Press, p. 507

Laurent, O., et al. 2000, A&A, 359, 887

Lehmer, B. D., Brandt, W. N., Hornschemeier, A. E., Alexander, D. M., Bauer, F. E., Koekemoer, A. M., Schneider, D. P., & Steffen, A. T. 2006. AJ, 131, 2394

Liu, Ji-Feng, Bregman, J. N. 2005, ApJS, 157, 59

Maloney, P. R., Hollenbach, D. J., & Tielens, A. G. G. M. 1996, ApJ, 466, 561

Martin, W. C., Sugar, J., Musgrove, A., Dalton, G. R., Wiese, W. L., & Fuhr, J. R. 1995, NIST Database for Atomic Spectroscopy, Version 2.0, NIST Standard Reference Database 61 (Gaithersburg: NIST)

Meijerink, R., & Spaans, M. 2005, A&A, 436, 397

Miller, C. M., & Colbert, E. J. M. 2004, Int. J. Mod. Phys. D, Vol. 13, No. 1, p. 1 (astro-ph/0308402)

Miller, J. M., Zezas, A., Fabbiano, G., & Schweizer, F. 2004, ApJ, 609, 728

Morris, P. W., et al. 2006, ApJ, 640, L179

Peeters, E., Spoon, H. W. W., & Tielens, A. G. G. M. 2004b, ApJ, 613, 986

Ptak, A. F., & Colbert, E. J. M. 2004, ApJ, 606, 291

Ptak, A., & Griffiths, R. 1999, ApJ, 517, 85

Roberts, T., et al. 2002, MNRAS, 337, 677

Roberts, T., & Warwick, R. 2000, MNRAS, 315, 98

Smith, J. D. T., et al. 2004 ApJS, 154, 159

Smith, J. D. T., et al. 2007 ApJ, accepted

Sturm, E., et al. 2002, A&A, 393, 821

Swartz, D. A., Ghosh, K. K., Tennant, A. F., & Wu, K. 2004, ApJ, 154, 519

Tully, R. B. 1988, Catalogue of Nearby Galaxies, Cambridge and New York, Cambridge University Press, 1988, p 221

Williams, R. M., Chu, Y. H., Gruendl, R. 2006, AJ, 132, 1877

Zezas, A., & Fabbiano, G. 2002b, ApJ, 577, 726

This 2-column preprint was prepared with the AAS LaTeX macros v5.2.

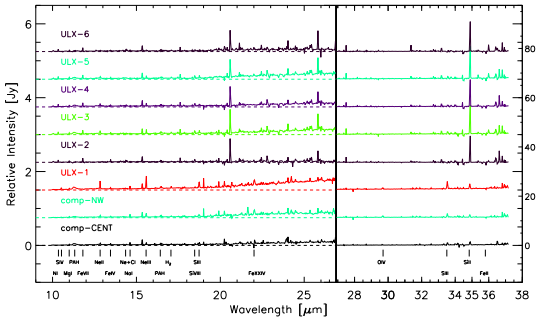

Fig. 1.— The combined spectra with the left SH and right LH modes for all of the sources analyzed in this study. For better visualization, the spectra have been plotted displaced along the y-axis. From $\sim$ 9 to $\sim$ 26.9 μm spectra are displaced by 0.75 Jy and $\sim$ 26.9 to $\sim$ 38 μm spectra are displaced by 15 Jy. Dashed lines are set to help indicate the slope of the continuum at wavelengths $\geq$ 20 μm.

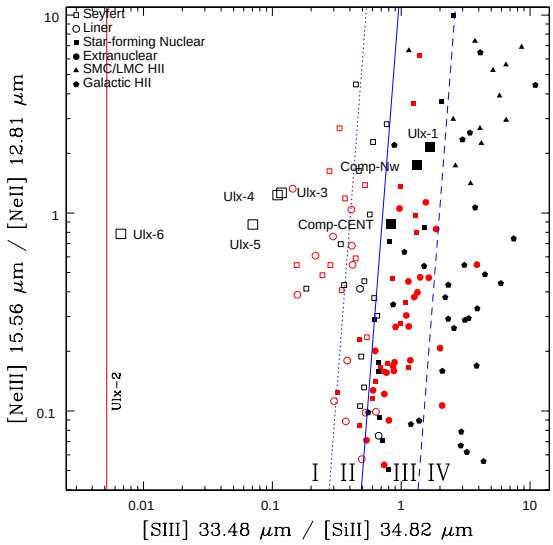

Fig. 2.— A neon, sulfur, and silicon diagnostic diagram showing line ratios for the eight regions in the NGC 4485/90 system (names in black). Nuclear and extra-nuclear regions from the sample of SINGS (Dale et al. 2006) are also plotted (in red) together with SMC, LMC and galactic H II regions. The red line for ULX-2 means that the value for the line ratio of [Ne III]15.55 μm/[Ne II]12.81 μm was not determined due to the undetected lines of Ne for this source. Zones III and IV are typical of SF-regions. Objects in zones I and II, can be classified as AGN-powered (Dale et al. 2006).

TABLE 1

THE LIST OF ULXS OF THE NGC 4485/90 SYSTEM TAKEN FROM ROBERTS ET AL. (2002).

ULX	RA (J2000)	DEC (J2000)	Notes	L_X[a] 10^{39} erg s^{-1}	T_{dust} [K]	τ[b] [10^{-10}]	$\tau_{9.7}$ [10^{-3}]
1	12:30:29.5	+41:39:27	NGC 4490 Radio Src. Possible SNR	1.0 (4.9)	50, 75, 200, 300	72000, 13000 0.1, 1.1	3310
2	12:30:30.6	+41:41:42	NGC 4485 X-1	4.0 (4.6)	135, 200	56, 2.3	4810
3	12:30:30.8	+41:39:11	NGC 4490 Transient X-ray Src.	2.9 (4.6)	90, 110	740, 240	3.93
4	12:30:32.3	+41:39:18	NGC 4490 X-1	1.9 (2.6)	75, 90	2500, 960	1.75
5	12:30:36.3	+41:38:37	NGC 4490 X-2	1.9 (2.6)	75, 90	8800, 16	7.94
6	12:30:43.2	+41:38:18	NGC 4490 X-4	3.1 (4.4)	75, 90 110, 135	360, 580 190, 10	2990

[a]Numbers in parenthesis give the intrinsic (unabsorbed) luminosity.

[b]The total extinction as a function of the extinction at 9.7 μm ($\tau_{9.7}$). The total extinction is modeled as a power low plus silicate features at 9.7 and 18 μm. The features are counted as a combination of measured galactic extinction profiles for these wavelengths (Smith et al. 2007).